



Influence of dc-bias on phase stability in Mn-doped Na 0.5 Bi 0.5 TiO 3 - 5.6 at . % BaTiO 3 single crystals

Wenwei Ge, Hu Cao, Jiefang Li, D. Viehland, Qinhui Zhang, and Haosu Luo

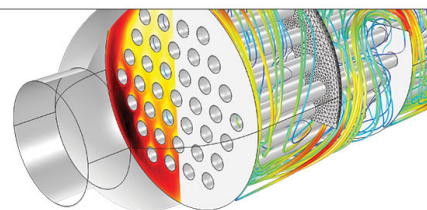
Citation: [Applied Physics Letters](#) **95**, 162903 (2009); doi: 10.1063/1.3253412

View online: <http://dx.doi.org/10.1063/1.3253412>

View Table of Contents: <http://scitation.aip.org/content/aip/journal/apl/95/16?ver=pdfcov>

Published by the [AIP Publishing](#)

Over **700** papers &
presentations on
multiphysics simulation



VIEW NOW ►

 COMSOL

Influence of dc-bias on phase stability in Mn-doped $\text{Na}_{0.5}\text{Bi}_{0.5}\text{TiO}_3$ -5.6 at. % BaTiO_3 single crystals

Wenwei Ge,^{1,a)} Hu Cao,¹ Jiefang Li,¹ D. Viehland,¹ Qinhui Zhang,² and Haosu Luo²

¹Department of Materials Science and Engineering, Virginia Tech, Blacksburg, Virginia 24061, USA

²Shanghai Institute of Ceramics, Chinese Academy of Sciences, Shanghai 201800, People's Republic of China

(Received 8 July 2009; accepted 1 October 2009; published online 20 October 2009)

Mn-doped $\text{Na}_{0.5}\text{Bi}_{0.5}\text{TiO}_3$ -5.6 at. % BaTiO_3 (Mn:NBT-5.6%BT) single crystals were grown by a top-seeded solution growth method. Tetragonal and rhombohedral phases were found to coexist in the as-grown condition. The dielectric and structural properties were studied as a function of temperature under dc electrical bias. An induced phase stability change from rhombohedral to tetragonal phases occurred under an electric-field applied along the $\langle 001 \rangle$ direction. © 2009 American Institute of Physics. [doi:10.1063/1.3253412]

Lead-free piezoelectric materials have attracted much attention in recent years from the view point of environmental protection.^{1,2} However, the piezoelectric performance of lead-free materials is still inferior to that of lead-containing ones thus determination of a mechanism by which to realize higher piezoelectricity in lead-free systems is an important topic at the present time. Since the time ultrahigh piezoelectric coefficients were first reported in oriented $(1-x)\text{Pb}(\text{Mg}_{1/3}\text{Nb}_{2/3}\text{O}_3)$ - $x\text{PbTiO}_3$ and $(1-x)\text{Pb}(\text{Zn}_{1/3}\text{Nb}_{2/3}\text{O}_3)$ - $x\text{PbTiO}_3$ crystals,³ many investigations have focused on monoclinic bridging phases around the morphotropic phase boundary (MPB).⁴⁻¹¹ Recently, a monoclinic M_C phase has been reported in $\langle 001 \rangle$ field-cooled BaTiO_3 single crystals,¹² indicating that ultrahigh piezoelectricity in Pb-free systems might be achieved via domain engineering.

Solid solutions of $(1-x)\text{Na}_{0.5}\text{Bi}_{0.5}\text{TiO}_3$ - $x\text{BaTiO}_3$ (abbreviated as NBT- x at.%BT) are potentially important lead-free piezoelectric materials, as they have a rhombohedral (R) to tetragonal (T) phase transition at a MPB near $0.06 < x < 0.08$. Accordingly, enhanced piezoelectric properties might be possible, if domain-engineered low symmetry states can be stabilized.¹³ However, electric field dependent phase transition studies of NBT- x at.%BT have not previously been reported, this may simply be because of difficulty in obtaining large single crystals of high resistance. Recently,¹⁴ the authors have developed Mn-doped NBT- x at.%BT (i.e., Mn:NBT-5.6at. %BT) crystals with notably higher resistivity, enabling near complete ferroelectric poling.

Here, in this letter, we report an investigation of the electric field dependence of the relative phase stability in $\langle 001 \rangle$ oriented Mn:NBT-5.6at. %BT single crystals. Our findings show an electric field induced R \rightarrow T phase stability change.

Single crystals of Mn:NBT- x at. %BT were grown by a top-seeded solution growth method from a 1 at. % Mn-doped $\text{Na}_{0.5}\text{Bi}_{0.5}\text{TiO}_3$ -10% BaTiO_3 solid flux. The concentration of Ba and Mn ions in the as-grown condition was determined by inductive coupled plasma atomic emission spectrometry to be 5.6 and 0.14 at. %, respectively. Pseudocubic $\langle 100 \rangle$ oriented Mn:NBT-5.6at. %BT crystal wafers with dimensions of $3 \times 3 \times 0.7$ mm³ were cut from the boule and sub-

sequently electroded on both surfaces with gold. Temperature dependent dielectric constant measurements were performed using a LCR meter (HP 4284A) under dc electric fields of $E=0, 8,$ and 12 kV/cm in the temperature range of 30 to 200 °C. Temperature dependent (200) line scans were taken using a Philips MPD high-resolution x-ray diffraction (XRD) system under fields of 0 and 11.4 kV/cm. The x-ray wavelength was that of $\text{Cu } K_\alpha = 1.5406$ Å and the x-ray generator was operated at 45 kV and 40 mA.

Figure 1 shows the temperature dependent dielectric constant ϵ_r and loss factor $\tan \delta$ for $\langle 100 \rangle$ oriented Mn:NBT-5.6at. %BT crystals taken on heating under $E=0, 8,$ and 12 kV/cm. Our investigations focused on a secondary ferroelectric transition in the range of 100 to 200 °C, which was below the dielectric maximum T_c at 280 °C. Below the secondary transition, the dielectric constant can be seen to become strongly frequency dispersive near 130 °C, somewhat analogous to that of relaxor ferroelectrics.²¹ Upon increasing the field, four observations can be made. First, the temperature of the secondary dielectric constant maximum was increased; from ~ 130 °C for $E=0$ kV/cm to ~ 150 °C for $E=12$ kV/cm. Second, the magnitude of the dielectric constant near this second maximum increased dramatically, from ~ 4000 for $E=0$ kV/cm to ~ 12000 for $E=12$ kV/cm. Third, for $E \geq 12$ kV/cm, the secondary transformation sharpened dramatically, becoming frequency independent. Fourth, for $E \geq 8$ kV/cm, a tertiary dielectric anomaly was found near 105 °C, indicating an additional step in the phase transformational sequence. Taken together, these data under different E indicate the following general trends. Under zero and moderate biases, the secondary phase transformation is diffuse. With increasing field, the transformation becomes gradually sharper and a tertiary step in the structural sequence becomes apparent. Near a critical bias, the diffuse characteristics are overridden and a sharp transition is induced; please note that there are similarities between this induced transition and the relaxor-to-normal transformation in relaxor ferroelectrics.^{22,23} After the dielectric measurements, we then cooled the Mn:NBT-5.6at. %BT crystal to room temperature at a rate of 2 °C/min under $E=12$ kV/cm applied along the $\langle 100 \rangle$. The piezoelectric d_{33} constant was then measured and determined to be 230 pC/N.

We next performed structural studies by XRD about the (200) and (220) zones at room temperature for as-grown

^{a)}Electronic mail: wenweige@vt.edu.

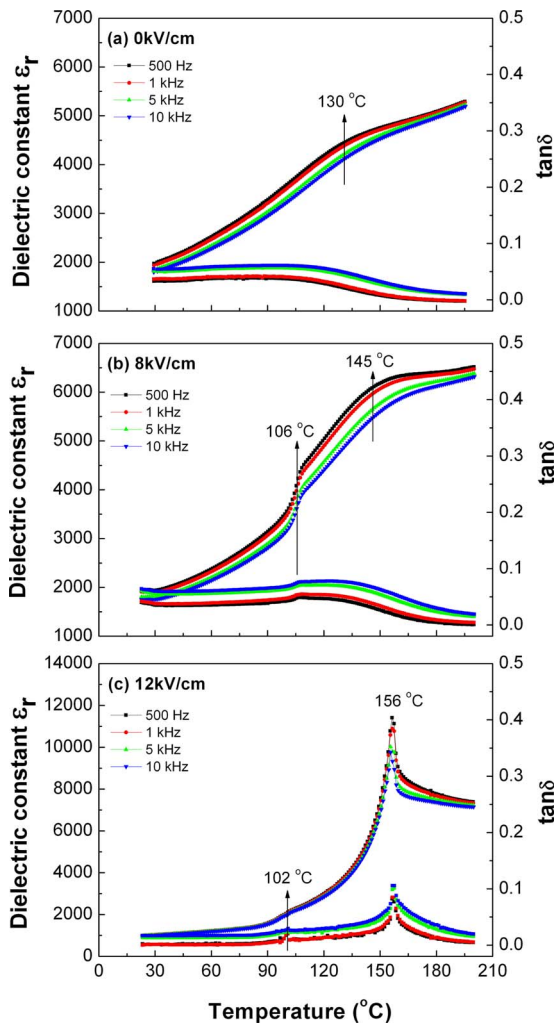


FIG. 1. (Color online) Temperature dependent dielectric constant ϵ_r and loss factor $\tan \delta$ for (100) oriented Mn:NBT-5.6%BT crystals taken heating under $E=0, 8,$ and 12 kV/cm.

Mn:NBT-5.6BT%. We annealed the crystal at 600 °C for 1 h and cooled to room temperature at a rate of 2 °C/min and again obtained (200) and (220) scans at room temperature. Finally, the crystal was heated to 200 °C and recooled to room temperature at a rate of 2 °C/min under dc biases of $E=6$ and 12 kV/cm, after which (200) and (220) scans were again obtained at room temperature. All of the XRD scans are given together in Fig. 2. The intensity is plotted on a logarithmic scale, so that small peaks with low intensity can be more clearly seen.

Along the pseudocubic (200) zone, an intense diffraction peak was found at $2\theta=46.51^\circ$ and a much weaker one was observed near $2\theta=46.01^\circ$; as can be seen in the left hand column of Fig. 2. Along the pseudocubic (220) zone, an intense peak was found at $2\theta=67.88^\circ$, which had two shoulders at $2\theta=67.68^\circ$ and 68.13° ; as can be seen in the right hand column of Fig. 2. Different rows show the results for different histories. The top row is for the as-grown condition; the second row for annealed; the third and final rows for the field cooled conditions under $E=6$ kV/cm and $E=12$ kV/cm, respectively. Comparisons of the various (200) and (220) scans will reveal that none of the diffraction peak positions were changed by thermal/electrical history. However, the intensity of the diffraction peaks was notably changed.

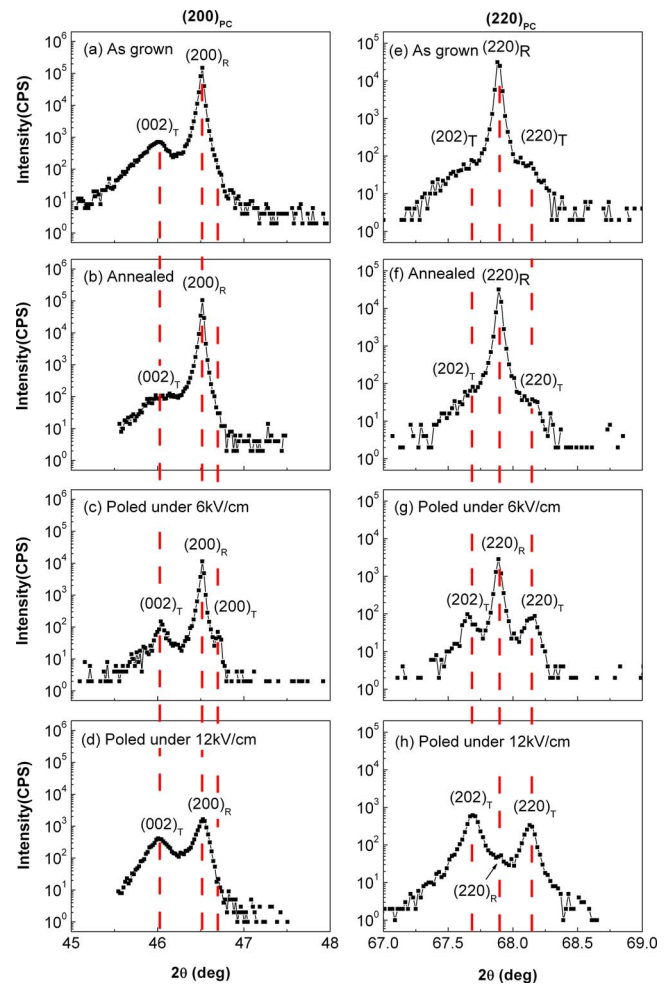


FIG. 2. (Color online) (200) and (220) x-ray line scans for Mn:NBT-5.6%BT crystals at room temperature: [(a) and (e)] as-grown crystal; [(b) and (f)] after annealing at 600 °C for 1 h; [(c) and (g)] after poling under dc $E=6$ kV/cm applied along $\langle 100 \rangle$ direction; [(d) and (h)] after poling under dc $E=12$ kV/cm applied along $\langle 100 \rangle$ direction.

We assign the intense peaks at $2\theta=46.51^\circ$ and 67.88° to the R phase. This is consistent with previously published phase diagrams,¹³ where Mn:NBT-5.6BT% can be expected to lie on the R side of the MPB ($6 < x < 7$ at. %). Generally, there should be both (220) and (111) splittings for the R phase. However, the rhombohedral distortion is very weak in NBT crystal,^{24,25} and thus its structure is very close to C. Accordingly, we could not find any splittings along (220) and (111) for either pure NBT or Mn:NBT-5.6BT% within the experimental accuracy of our system; perhaps high energy synchrotron XRD studies are needed in the future. The other diffraction peaks in Fig. 2 can be assigned to the T phase. The lattice parameters were determined to be $(a_r, \alpha) = (3.9020 \text{ \AA}, 89.98^\circ)$ and $(a_t, c_t) = (3.8897, 3.9421) \text{ \AA}$ for the R and T phases, respectively. Please note that these lattice constants were determined using both (200) and (220) scans, and that they were consistent with each other. These results show that the T and R phases coexist in Mn:NBT-5.6at. %BT: the composition lies close to the MPB (Ref. 13) ($6 < x < 7$ at. %) between R and T phases, but the R phase is dominant. Furthermore, from the lattice parameters, we calculated that a huge volume change of 0.39% must occur at the $R \rightarrow T$ phase stability change.

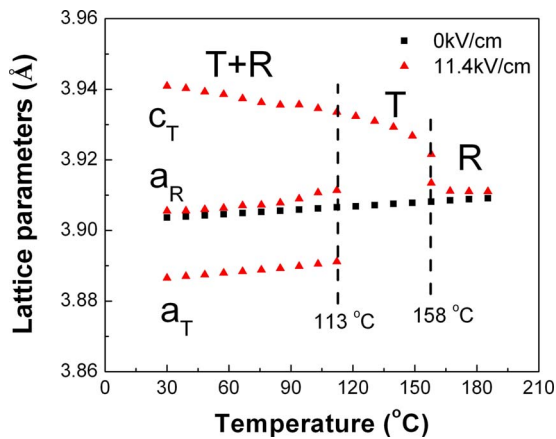


FIG. 3. (Color online) Temperature dependence of the crystal lattice parameters for Mn:NBT-5.6%BT under field of $E=0$ and 11.4 kV/cm.

Interestingly, the (200) pseudocubic reflection exhibited a large increase in the $(200)_r/(002)_t$ intensity ratio from 212 before annealing to 974 after annealing. This may result from one of two reasons. First, the R/T phase volume ratio might be increased by annealing. Since Mn:NBT-5.6at %BT lies close to the MPB, the T and R phases should be energetically close and thus there might be some metastability with thermal/electrical history. Second, the domain population might be altered by annealing; if this is the case, then we can conclude that the a-domain state is favored by annealing. Such a 90° domain switching by annealing might be explained by a “symmetry-conforming principle” of point defects, which was first proposed in ferroelastic/martensite.^{15–17} This model was later extended to BaTiO₃-based ferroelectrics^{18–20} and used to explain reversible ferroelectric domain-switching in aged samples, in particular Mn-doped perovskite.^{18–20} We note also near the MPB that the conforming-symmetry of the internal fields of point defects might alter slightly the relative R/T phase stability.

After field-cooling under $E=6$ kV/cm applied along the (001), the intensity for the T peaks was notably increased, whereas that of the R peaks was decreased: as can be seen in Figs. 2(c) and 2(g). With increase of E to 12 kV/cm, the intensity of the $(200)_r$ peak was further notably decreased, whereas that for the $(220)_r$ had nearly disappeared: as can be seen in Figs. 2(d) and 2(h). These results clearly demonstrate a change from R to T phase stability between as-grown and field-cooled conditions, although T was clearly present in both conditions.

Next, we measured the temperature dependence of the crystal lattice parameters under $E=0$ and 11.4 kV/cm applied along the (001). We began the investigations from the annealed condition. The results are shown in Fig. 3. For $E=0$ kV/cm, an intense (200) peak for the R phase was observed, whose lattice parameter increased near linearly with temperature. Under zero-field, the R phase was dominant, whereas the peak for the T phase was so weak that its position could not be determined with accuracy thus the lattice parameters for the T phase under zero-field are not shown in Fig. 3. However, in the field heating condition between 30 and 113 °C under $E=11.4$ kV/cm, the (200) and (220) reflections exhibited an obvious T splitting. Both T and R phases were found on heating in this temperature range, with

lattice parameters as given in Fig. 3. On heating between 113 and 158 °C under $E=11.4$ kV/cm, the (200) pseudocubic reflection exhibited only the (002) peak for the T phase. This indicates that Mn:NBT-5.6%BT transforms into a near single c-domain T state under $E \geq 11.4$ kV/cm in this temperature range. The lattice parameter a_t was not given in the temperature range of 113 to 158 °C because we could not obtain a_t along the zones we had access to for a single c-domain Mn:NBT-5.6%BT wafer with thickness of 0.7 mm. Clearly, the tertiary phase transition observed in the dielectric constant [see Figs. 1(b) and 1(c)] is related to contributions from T domain realignment. In addition, near 158 °C, an abrupt phase transition occurred and the lattice parameters were equivalent to that for the R phase under $E=0$. This indicates that the Mn:NBT-5.6at. %BT crystal may have underwent a phase transition from single domain T ferroelectric to anti-ferroelectric, as previously suggested.¹³

In summary, the relative phase stability of Mn:NBT-5.6at. %BT crystals was investigated under dc electrical bias. T and R phases were found to coexist in the as-grown condition, with the R phase being dominant. With increasing temperature, an induced relative phase stability change from R to T phases was observed for an E-field applied along $\langle 001 \rangle$. Our results demonstrate that this T phase remains stable after removal of E in the field-cooled state.

This work was supported by the National Science Foundation (Materials world network) under Grant No. DMR-0806592, by the Department of Energy under Grant No. DE-FG02-07ER46480, by the Natural Science Foundation of China under Grant No. 50602047, and by the Shanghai Municipal Government Grant No. 08JC1420500.

¹E. Cross, *Nature (London)* **432**, 24 (2004).

²Y. Saito, H. Takao, T. Tani, T. Nonoyama, K. Takatori, T. Homma, T. Nagaya, and M. Nakamura, *Nature (London)* **432**, 84 (2004).

³S.-E. Park and T. R. Shrout, *J. Appl. Phys.* **82**, 1804 (1997).

⁴B. Noheda, D. Cox, G. Shirane, J. Gonzalo, L. Cross, and S. Park, *Appl. Phys. Lett.* **74**, 2059 (1999).

⁵B. Noheda, D. E. Cox, G. Shirane, S. Park, L. Cross, and Z. Zhong, *Phys. Rev. Lett.* **86**, 3891 (2001).

⁶D. Vanderbilt and M. Cohen, *Phys. Rev. B* **63**, 094108 (2001).

⁷Z.-G. Ye, B. Noheda, M. Dong, D. Cox, and G. Shirane, *Phys. Rev. B* **64**, 184114 (2001).

⁸A. Singh and D. Pandey, *Phys. Rev. B* **67**, 064102 (2003).

⁹C. Tu, I. Shih, V. Schmidt, and R. Chien, *Appl. Phys. Lett.* **83**, 1833 (2003).

¹⁰H. Cao, F. Bai, N. Wang, J. Li, D. Viehland, G. Xu, and G. Shirane, *Phys. Rev. B* **72**, 064104 (2005).

¹¹M. Ahart, M. Somayazulu, R. E. Cohen, P. Ganesh, P. Dera, H. Mao, R. J. Hemley, Y. Ren, P. Liermann, and Z. Wu, *Nature (London)* **451**, 545 (2008).

¹²H. Cao, C. Devreugd, W. Ge, J. Li, D. Viehland, X. Zhao, and H. Luo, *Appl. Phys. Lett.* **94**, 032901 (2009).

¹³T. Takenaka, K. Maruyama, and K. Sakata, *Jpn. J. Appl. Phys., Part 1* **30**, 2236 (1991).

¹⁴Q. Zhang, Y. Zhang, F. Wang, Y. Wang, D. Lin, X. Zhao, H. Luo, W. Ge, and D. Viehland, *Appl. Phys. Lett.* **95**, 102904 (2009).

¹⁵X. Ren and K. Otsuka, *Nature (London)* **389**, 579 (1997).

¹⁶X. Ren and K. Otsuka, *Phys. Rev. Lett.* **85**, 1016 (2000).

¹⁷X. Ren and K. Otsuka, *MRS Bull.* **27**, 115 (2002).

¹⁸X. Ren, *Nature Mater.* **3**, 91 (2004).

¹⁹L. Zhang and X. Ren, *Phys. Rev. B* **73**, 094121 (2006).

²⁰L. X. Zhang, W. Chen, and X. Ren, *Appl. Phys. Lett.* **85**, 5658 (2004).

²¹D. Viehland, M. Wuttig, and L. E. Cross, *J. Appl. Phys.* **68**, 2916 (1990).

²²X. H. Dai, Z. Xu, and D. Viehland, *Philos. Mag. B* **70**, 33 (1994).

²³H. Cao, J. Li, and D. Viehland, *J. Appl. Phys.* **100**, 034110 (2006).

²⁴S. Park and S. Chung, *J. Am. Ceram. Soc.* **77**, 2641 (1994).

²⁵S. Park, S. Chung, and I. Kim, *J. Am. Ceram. Soc.* **79**, 1290 (1996).